Research Article | Vol. 7, No. 3 | 1 Mar 2017 | OPTICAL MATERIALS EXPRESS 1105

Optical Materials EXPRESS

Effect of silver nanowire length in a broad range on optical and electrical properties as a transparent conductive film

MIKITA MARUS,[1,2] ALIAKSANDR HUBAREVICH,[1] REUBEN JEREMY WEIXIONG LIM,[2] HUI HUANG,[2,5] ALIAKSANDR SMIRNOV,[3] HONG WANG,[1] WEIJUN FAN,[1,6] AND XIAO WEI SUN[4,*]

[1]*School of Electrical and Electronic Engineering, Nanyang Technological University, 50 Nanyang Avenue, 639798, Singapore*
[2]*Singapore Institute of Manufacturing Technology, 71 Nanyang Drive, 638075, Singapore*
[3]*Department of Micro- and Nanoelectronics, Belarusian State University of Informatics and Radioelectronics, 6 P. Brovki, Minsk 220013, Belarus*
[4]*Department of Electrical and Electronic Engineering, College of Engineering, South University of Science and Technology, 1088 Xue-Yuan Road, Nanshan, Shenzhen, Guangdong 518055, China*
[5]*hhuang@SIMTech.a-star.edu.sg*
[6]*EWJFan@ntu.edu.sg*
**sunxw@sustc.edu.cn*

Abstract: Optical and electrical properties of silver nanowire transparent conductive films with a broad range of nanowire lengths were studied. A proposed simulation model demonstrated similar behavior with experimental results for 30 and 90 μm nanowires, and thus it was used to expand the range of nanowire lengths from 10 to 200 μm. Theoretical results show that a lengthening of silver nanowires results in an increase of their optoelectronic performance; 200 μm long nanowire possess 13.5 times lower sheet resistance compared to 10 μm ones, while the transmittance remains similar for coverage densities of nanowires up to 25%. Moreover, the dependence of the sheet resistance on the length of nanowires changes *non-linearly*; from 10 to 20 μm, 20 to 80 μm and 80 to 200 μm the sheet resistance drops by a factor of 5, 2.25 and 1.2 respectively. Furthermore, a thickening of nanowire diameters from 30 to 90 nm decreases the sheet resistance to 5.8 times. Obtained results allow a deeper analysis of the silver nanowire transparent conductive films from the perspective of the length of nanowires for various optoelectronic applications.

OCIS codes: (310.7005) Transparent conductive coatings; (350.4238) Nanophotonics and photonic crystals.

References and links

1. S. Kang, T. Kim, S. Cho, Y. Lee, A. Choe, B. Walker, S.-J. Ko, J. Y. Kim, and H. Ko, "Capillary Printing of Highly Aligned Silver Nanowire Transparent Electrodes for High-Performance Optoelectronic Devices," Nano Lett. **15**(12), 7933–7942 (2015).
2. T. H. Seo, A. H. Park, S. Park, S. Chandramohan, G. H. Lee, M. J. Kim, C.-H. Hong, and E.-K. Suh, "Improving the graphene electrode performance in ultra-violet light emitting diode using silver nanowire networks," Opt. Mater. Express **5**(2), 314–322 (2015).
3. D. Paeng, J. H. Yoo, J. Yeo, D. Lee, E. Kim, S. H. Ko, and C. P. Grigoropoulos, "Low-cost facile fabrication of flexible transparent copper electrodes by nanosecond laser ablation," Adv. Mater. **27**(17), 2762–2767 (2015).
4. P. B. Catrysse and S. Fan, "Nanopatterned metallic films for use as transparent conductive electrodes in optoelectronic devices," Nano Lett. **10**(8), 2944–2949 (2010).
5. H. Lee, S. Hong, K. Yang, and K. Choi, "Fabrication of 100nm metal lines on flexible plastic substrate using ultraviolet curing nanoimprint lithography," Appl. Phys. Lett. **88**(14), 143112 (2006).
6. M. Layani, A. Kamyshny, and S. Magdassi, "Transparent conductors composed of nanomaterials," Nanoscale **6**(11), 5581–5591 (2014).
7. J. van de Lagemaat, T. M. Barnes, G. Rumbles, S. E. Shaheen, T. J. Coutts, C. Weeks, I. Levitsky, J. Peltola, and P. Glatkowski, "Organic solar cells with carbon nanotubes replacing In2O3:Sn as the transparent electrode," Appl. Phys. Lett. **88**(23), 233503 (2006).
8. G.-J. Jeong, J.-H. Lee, S.-H. Han, W.-Y. Jin, J.-W. Kang, and S.-N. Lee, "Silver nanowires for transparent conductive electrode to GaN-based light-emitting diodes," Appl. Phys. Lett. **106**(3), 031118 (2015).

#283836 https://doi.org/10.1364/OME.7.001105
Journal © 2017 Received 29 Dec 2016; revised 11 Feb 2017; accepted 21 Feb 2017; published 27 Feb 2017

Optical Materials EXPRESS

9. Q. G. Du, K. Sathiyamoorthy, L. P. Zhang, H. V. Demir, C. H. Kam, and X. W. Sun, "A two-dimensional nanopatterned thin metallic transparent conductor with high transparency from the ultraviolet to the infrared," Appl. Phys. Lett. **101**(18), 181112 (2012).
10. K. Ghaffarzadeh and R. Das, "Transparent conductive films (TCF) 2016-2026: forecasts, markets, technologies," http://www.idtechex.com/research/reports/transparent-conductive-films-tcf-2016-2026-forecasts-markets-technologies-000480.asp
11. J. H. Maurer, L. González-García, B. Reiser, I. Kanelidis, and T. Kraus, "Templated self-assembly of ultrathin gold nanowires by nanoimprinting for transparent flexible electronics," Nano Lett. **16**(5), 2921–2925 (2016).
12. C. J. M. Emmott, A. Urbina, and J. Nelson, "Environmental and economic assessment of ITO-free electrodes for organic solar cells," Sol. Energy Mater. Sol. Cells **97**, 14–21 (2012).
13. S. Nam, M. Song, D.-H. Kim, B. Cho, H. M. Lee, J.-D. Kwon, S.-G. Park, K.-S. Nam, Y. Jeong, S.-H. Kwon, Y. C. Park, S.-H. Jin, J.-W. Kang, S. Jo, and C. S. Kim, "Ultrasmooth, extremely deformable and shape recoverable Ag nanowire embedded transparent electrode," Sci. Rep. **4**, 4788 (2014).
14. A. Hubarevich, M. Marus, W. Fan, A. Smirnov, X. W. Sun, and H. Wang, "Theoretical comparison of optical and electronic properties of uniformly and randomly arranged nano-porous ultra-thin layers," Opt. Express **23**(14), 17860–17865 (2015).
15. W.-G. Yan, Z.-B. Li, and J.-G. Tian, "Tunable fabrication and optical properties of metal nano hole arrays," J. Nanosci. Nanotechnol. **15**(2), 1704–1707 (2015).
16. A. Hubarevich, M. Marus, A. Stsiapanau, A. Smirnov, J. Zhao, W. Fan, H. Wang, and X. Sun, "Transparent conductive nanoporous aluminium mesh prepared by electrochemical anodizing," Phys. Status Solidi., A Appl. Mater. Sci. **212**(10), 2174–2178 (2015).
17. A. R. Rathmell, S. M. Bergin, Y. L. Hua, Z. Y. Li, and B. J. Wiley, "The growth mechanism of copper nanowires and their properties in flexible, transparent conducting films," Adv. Mater. **22**(32), 3558–3563 (2010).
18. J. V. Coe, J. M. Heer, S. Teeters-Kennedy, H. Tian, and K. R. Rodriguez, "Extraordinary transmission of metal films with arrays of subwavelength holes," Annu. Rev. Phys. Chem. **59**(1), 179–202 (2008).
19. D.-H. Kim, K.-C. Yu, Y. Kim, and J.-W. Kim, "Highly stretchable and mechanically stable transparent electrode based on composite of silver nanowires and polyurethane-urea," ACS Appl. Mater. Interfaces **7**(28), 15214–15222 (2015).
20. J. W. Lim, Y. T. Lee, R. Pandey, T.-H. Yoo, B.-I. Sang, B.-K. Ju, D. K. Hwang, and W. K. Choi, "Effect of geometric lattice design on optical/electrical properties of transparent silver grid for organic solar cells," Opt. Express **22**(22), 26891–26899 (2014).
21. D. S. Hecht, L. Hu, and G. Irvin, "Emerging transparent electrodes based on thin films of carbon nanotubes, graphene, and metallic nanostructures," Adv. Mater. **23**(13), 1482–1513 (2011).
22. J. Gao, K. Kempa, M. Giersig, E. M. Akinoglu, B. Han, and R. Li, "Physics of transparent conductors," Adv. Phys. **65**(6), 553–617 (2016).
23. Y.-H. Ho, K.-Y. Chen, S.-W. Liu, Y.-T. Chang, D.-W. Huang, and P.-K. Wei, "Transparent and conductive metallic electrodes fabricated by using nanosphere lithography," Org. Electron. **12**(6), 961–965 (2011).
24. L. Zhang, J. Hao, H. Ye, S. P. Yeo, M. Qiu, S. Zouhdi, and C.-W. Qiu, "Theoretical realization of robust broadband transparency in ultrathin seamless nanostructures by dual blackbodies for near infrared light," Nanoscale **5**(8), 3373–3379 (2013).
25. G.-Q. Liu, Y. Hu, Z.-Q. Liu, Y.-H. Chen, Z.-J. Cai, X.-N. Zhang, and K. Huang, "Robust multispectral transparency in continuous metal film structures via multiple near-field plasmon coupling by a finite-difference time-domain method," Phys. Chem. Chem. Phys. **16**(9), 4320–4328 (2014).
26. Z.-Q. Liu, G.-Q. Liu, H.-Q. Zhou, X.-S. Liu, K. Huang, Y.-H. Chen, and G.-L. Fu, "Near-unity transparency of a continuous metal film via cooperative effects of double plasmonic arrays," Nanotechnology **24**(15), 155203 (2013).
27. Z. Liu, Y. Nie, W. Yuan, X. Liu, S. Huang, J. Chen, H. Gao, G. Gu, and G. Liu, "Optical cavity-assisted broadband optical transparency of a plasmonic metal film," Nanotechnology **26**(18), 185701 (2015).
28. Z.-Q. Liu, G.-Q. Liu, K. Huang, Y.-H. Chen, Y. Hu, X.-G. Zhang, and Z.-Q. Cai, "Enhanced Optical Transmission of a Continuous Metal Film With Double Metal Cylinder Arrays," IEEE Photonics Technol. Lett. **25**(12), 1157–1160 (2013).
29. W.-G. Yan, Z.-B. Li, and J.-G. Tian, "Tunable fabrication and optical properties of metal nano hole arrays," J. Nanosci. Nanotechnol. **15**(2), 1704–1707 (2015).
30. M. Marus, A. Hubarevich, H. Wang, A. Stsiapanau, A. Smirnov, X. W. Sun, and W. Fan, "Comparative analysis of opto-electronic performance of aluminium and silver nano-porous and nano-wired layers," Opt. Express **23**(20), 26794–26799 (2015).
31. M. Jagota and N. Tansu, "Conductivity of nanowire arrays under random and ordered orientation configurations," Sci. Rep. **5**, 10219 (2015).
32. M. Marus, A. Hubarevich, H. Wang, A. Smirnov, X. Sun, and W. Fan, "Optoelectronic performance optimization for transparent conductive layers based on randomly arranged silver nanorods," Opt. Express **23**(5), 6209–6214 (2015).
33. M. Marus, A. Hubarevich, H. Wang, Y. Mukha, A. Smirnov, H. Huang, W. Fan, and X. W. Sun, "Towards theoretical analysis of optoelectronic performance of uniform and random metallic nanowire layers," Thin Solid Films **626**, 140–144 (2016).

Optical Materials EXPRESS

34. C. Preston and L. Hu, "Silver nanowires," in *Handbook of Visual Display Technology*, J. Chen, W. Cranton, and M. Fihn, (Springer, 2016).
35. Y. Sun and Y. Xia, "Large-scale synthesis of uniform silver nanowires through a soft, self-seeding, polyol process," Adv. Mater. **14**(11), 833–837 (2002).
36. F. N. Kholid, H. Huang, Y. Zhang, and H. J. Fan, "Multiple electrical breakdowns and electrical annealing using high current approximating breakdown current of silver nanowire network," Nanotechnology **27**(2), 025703 (2016).
37. Lumerical FDTD Solutions, Available from: *https://www.lumerical.com/tcad-products/fdtd/*.
38. E. D. Palik, *Handbook of Optical Constants of Solids*, (Academic, 1998).
39. B. Last and D. Thouless, "Percolation theory and electrical conductivity," Phys. Rev. Lett. **27**(25), 1719–1721 (1971).
40. J. Fitzpatrick, R. Malt, and F. Spaepen, "Percolation theory and the conductivity of random close packed mixtures of hard spheres," Phys. Lett. A **47**(3), 207–208 (1974).
41. S. Kirkpatrick, "Percolation and conduction," Rev. Mod. Phys. **45**(4), 574–588 (1973).
42. J. van de Groep, P. Spinelli, and A. Polman, "Transparent conducting silver nanowire networks," Nano Lett. **12**(6), 3138–3144 (2012).
43. L. Hu, H. Wu, and Y. Cui, "Metal nanogrids, nanowires, and nanofibers for transparent electrodes," MRS Bull. **36**(10), 760–765 (2011).
44. S. Xie, Z. Ouyang, B. Jia, and M. Gu, "Large-size, high-uniformity, random silver nanowire networks as transparent electrodes for crystalline silicon wafer solar cells," Opt. Express **21**(103), A355–A362 (2013).
45. M. Rycenga, C. M. Cobley, J. Zeng, W. Li, C. H. Moran, Q. Zhang, D. Qin, and Y. Xia, "Controlling the synthesis and assembly of silver nanostructures for plasmonic applications," Chem. Rev. **111**(6), 3669–3712 (2011).
46. D. Y. Choi, H. W. Kang, H. J. Sung, and S. S. Kim, "Annealing-free, flexible silver nanowire-polymer composite electrodes via a continuous two-step spray-coating method," Nanoscale **5**(3), 977–983 (2013).
47. W. L. Barnes, A. Dereux, and T. W. Ebbesen, "Surface plasmon subwavelength optics," Nature **424**(6950), 824–830 (2003).
48. M. Aryal, J. Geddes, O. Seitz, J. Wassei, I. McMackin, and B. Kobrin, ""Sub-micron transparent metal mesh conductor for touch screen displays," in SID Symposium," Dig. Tech. Pap. **45**(1), 194–196 (2014).
49. B.-Y. Wang, T.-H. Yoo, J. W. Lim, B.-I. Sang, D.-S. Lim, W. K. Choi, D. K. Hwang, and Y. J. Oh, "Enhanced light scattering and trapping effect of Ag nanowire mesh electrode for high efficient flexible organic solar cell," Small **11**(16), 1905–1911 (2015).

1 Introduction

Transparent conductive films (TCFs) remain an inevitable component of many optoelectronic devices such as liquid crystal displays, solar cells, touchscreens, light-emitting diodes and others [1–9]. TCFs based on indium tin oxide (ITO) still dominate within electronics industry [10]. However, the fragility of the ITO films limits its usage in flexible optoelectronics [11], regardless of other drawbacks such as high fabrication cost [12]. Metallic patterned TCFs offer competitive optical and electrical properties and flexibility required for most trending optoelectronic devices [13–19]. Furthermore, geometrical configuration [20–23], plasmon resonances and strong near-field coupling effects [24–28] of metallic patterned TCFs significantly affects their transmittance and sheet resistance. Latest research demonstrates an advantage of the nanowire TCFs in comparison with porous and triangle configurations of patterns [29, 30]. Moreover, randomly arranged nanowires (NWs) can exhibit optoelectronic performance comparable to uniform nanoscale networks [31–33] and benefit from low cost non-lithographic fabrication processes making them a preferable candidate for a future generation of flexible TCFs.

Recent research demonstrated that TCFs with longer NWs possess higher optoelectronic performance [34]. However, a clear impact of their length in broad range on the transmittance and sheet resistance, which are the two critical indexes of the TCFs, is poorly studied. Herein we investigated the optoelectronic performance of silver NW (AgNW) films for the NW lengths from 10 to 200 μm. We found that a lengthening of AgNWs results in increase of their optoelectronic performance: 200 μm long NWs possess 10 times lower sheet resistance compared to 10 μm ones, while the transmittance remains similar for coverage densities of NWs up to 25%. Moreover, the dependence of the sheet resistance on the length of NWs changes *non-linearly*: from 10 to 20 μm, 20 to 80 μm and 80 to 200 μm the sheet resistance drops by a factor of 5, 2.25 and 1.2 respectively. Our results explain the influence of NW

Optical Materials EXPRESS

length in broad range on the optical and electrical properties of AgNW TCFs and grant the opportunity to deepen their analysis for various optoelectronic applications such as displays, solar cells, light-emitting diodes, touch screens and smart windows.

2 Methodology

2.1 Synthesis of AgNWs

We fabricated AgNWs at 160° C in an automated synthesis chamber using the well-known polyol process [35]. Silver nitrate ($AgNO_3$), ethylene glycol (EG), copper chloride and polyvinylpyrrolidone (PVP) were used as starting materials, and the synthesis processes are detailed elsewhere [36]. Requirements for lengths and diameters of AgNWs were met through controlling the reaction parameters of polyol synthesis. The as-synthesized AgNWs were cleaned three times in isopropanol (IPA) and then re-dispersed in deionized (DI) water.

2.2 Fabrication of the AgNW TCFs

AgNW ink was formulated at 3 mg/ml Ag concentration in DI water. The AgNW ink was coated over a 150 mm-width polyethylene terephthalate (PET) flexible substrate on a Coatema roll-to-roll (R2R) smart coater with a slot-die at a coating speed of 0.2 m/min and was dried at 150° C. AgNW loading density (LD) was controlled by adjusting the ink feeding rate to the slot-die coater. The as-coated films were cut into 5 cm by 5 cm samples for characterization. Sheet resistance was measured using a Delcom Instruments benchtop contactless probe. Optical measurements were performed using BYK-Gardner Haze-Gard I for wavelength range 400-800 nm.

2.3 Simulation

Figure 1 shows the geometrical models representing metallic NW films with different length of NWs. Cylindrical NWs were randomly spread across a PET substrate according to the following steps: (i) initially, NWs were uniformly arranged; (ii) then, each NW was arbitrarily shifted along *X* and *Y* axes for distances ranging from -*L* to *L*, where *L* is the length of NWs; (iii) and finally, each NW was arbitrarily rotated within *X* and *Y* axes for an angle ranging from –90 to 90 degrees.

A commercial-grade simulator based on the finite-difference time-domain (FDTD) method was used to perform the optical calculations [37]. The index of refraction *n* and extinction coefficient *k* was used from [38]. The incident light in range from 400 to 800 nm was distributed along *Z* axis. The periodic boundary conditions and perfectly matched films were applied perpendicular and parallel to *Z* axis, respectively. Mesh size was set to 10, 10 and 5 nm in *X*, *Y*, and *Z* directions, respectively. Each arrangement of AgNWs was simulated three times for arbitrarily chosen position of 15 × 15 μm^2 simulation area (red areas in Fig. 1) in order to justify the reproducibility of optical properties.

Sheet resistance was calculated by percolation model in accordance with [39,40] which is given by the following equation:

$$R_{sh} = \frac{1}{h\sigma_0 \left(\phi_f - \phi_{crit}\right)^t}, \tag{1}$$

where σ_0 is the conductivity of metal, ϕ_f is the volume fraction of patterned metal film, ϕ_{crit} is the volume fraction threshold when the patterned film changes from insulator to conductor, *h* is the thickness of the metal film and *t* is the critical exponent.

The subtraction of ϕ_{crit} from ϕ_f for randomly arranged NW films is expressed as follows [32]:

Optical Materials EXPRESS

$$\phi_f - \phi_{crit} = \frac{\left(\left\langle N_i^* \right\rangle - N_{crit}\right) V_c}{V_{uc}}, \tag{2}$$

where $\left\langle N_i^* \right\rangle$ is the effective number of the NW crossings which contributes to the conductivity of the NW films, N_{crit} is the critical number of the NW crossings when the NW film changes from insulator to conductor, V_c is the NW crossings volume and V_{uc} is the unit cell volume.

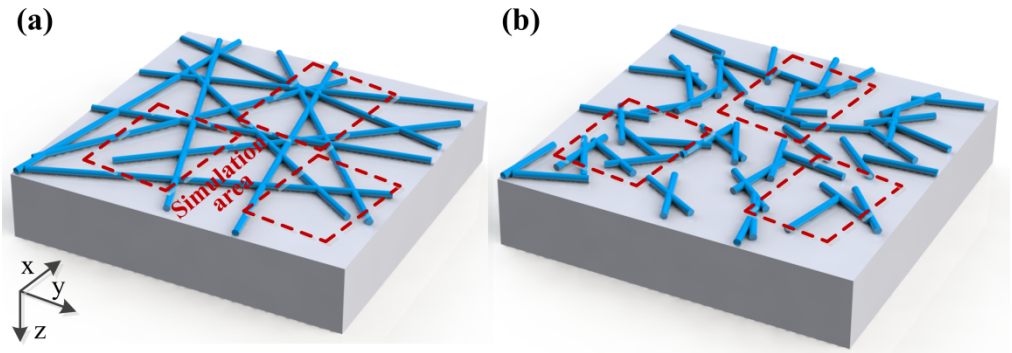

Fig. 1. Geometrical models of metallic NW films with different length of NWs on PET substrate. Red rectangles represent 15 × 15μm^2 unit simulation areas.

Above mentioned models were proved to be in good agreement with experimental data and successfully applied by our group in previous works [30, 32, 33].

3 Results and discussion

Randomly arranged AgNWs with diameters of 30, 60 and 90 nm and length from 10 to 60 μm are commonly used in experimental studies [42–46]. We used AgNWs with diameter of 60 nm, lengths of 30 and 90 μm and coverage density *D* in range from 5 to 25% for experimental part of our study. Figure 2 shows the dependence of transmittance on sheet resistance of AgNW TCFs with different lengths of AgNWs. The film fabricated from AgNWs with an average length of 30 μm possessed the transmittance of 76% at the sheet resistance of 20 Ohm/sq, while the film made from longer AgNWs of 90 μm [shown in SEM image in Fig. 2(b)] – higher transmittance of 82% at the same sheet resistance. Simulation results demonstrated similar behavior for these lengths, which indicated a feasibility of the proposed theoretical model. In order to further investigate the influence of length of AgNW on the optoelectronic properties of AgNW films we expanded the range of AgNW lengths from 10 to 200 μm and coverage density *D* in range from 5 to 50%. The transmittance of TCFs with short 10 μm NWs decreased by 9% compared to 30 μm NWs at same sheet resistance of 20 Ohm/sq. Surprisingly, the transmittance of 200 μm long NWs increased by only 3% compared to 90 μm NWs for the films with same sheet resistance and equals to 85%. Thus, a uniform growth of AgNW length results in a *non-linear* increase of the optoelectronic performance: (i) + 9% transmittance from 10 to 30 μm, (ii) + 6% transmittance from 30 to 90 μm and (iii) only + 3% transmittance from 90 to 200 μm at 20 Ohm/sq sheet resistance. Based on the above mentioned observations we decided to broaden the theoretical investigation of the influence of NW length on the transmittance and sheet resistance independently.

Optical Materials EXPRESS

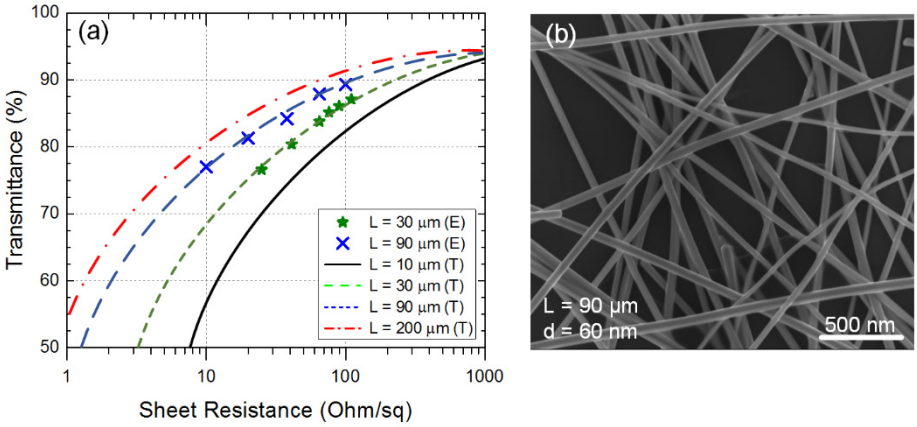

Fig. 2. (a) Transmittance at 550 nm against the sheet resistance for different lengths of AgNWs. The diameter of NWs is 60 nm for both experimental (*E*) and theoretical (*T*) data. (b) SEM image for AgNWs with length L = 90 mm and diameter d = 60 nm.

Figure 3(a) shows the transmittance spectra of AgNW films for various coverage densities D and lengths L of NWs. The transmittance decreases in range from 400 to 475 nm due to localized surface plasmon resonance and keeps almost uniform till 800 nm [30, 46]. The transmittance at 550 nm for D = 6% equals to 93% for both 200 and 10 µm long NWs. At D = 25% the transmittance decreases down to 73% and 71% for 200 and 10 µm long NWs, respectively. The optical difference between these lengths attributes to surface plasmon polaritons (SPPs), which excite and propagate along the NWs. 10 µm long NWs result in shorter distances between consequent NW crossings, and thus in larger amount of localized electric field areas as shown in Fig. 3(b). Therefore, 10 µm NWs possess a shorter propagation length of SPPs and less influence on the transmittance correspondingly. The average transmittance at D = 40% decreases down to 57% and 52% for 200 and 10 µm long NWs, respectively. The distances between consequent NW crossings for 10 µm NWs at such high coverage density result in negligibly low influence of the SPPs on the transmittance. In contrast to AgNW TCFs, the aluminum NW (AlNW) films – possessing weak SP response from 400 to 500 nm – show negligible difference between 200 and 10 µm long NWs for all above mentioned coverage densities D as shown in Fig. 3(c). Since TCFs for most optoelectronic devices require the transmittance above 80%, we can conclude that the length of NWs insignificantly affects the optical performance. Nevertheless, in case of devices satisfied with TCFs having transmittance below 80% long metallic NWs with strong SP response possess higher transmittance than shorter NWs.

Optical Materials EXPRESS

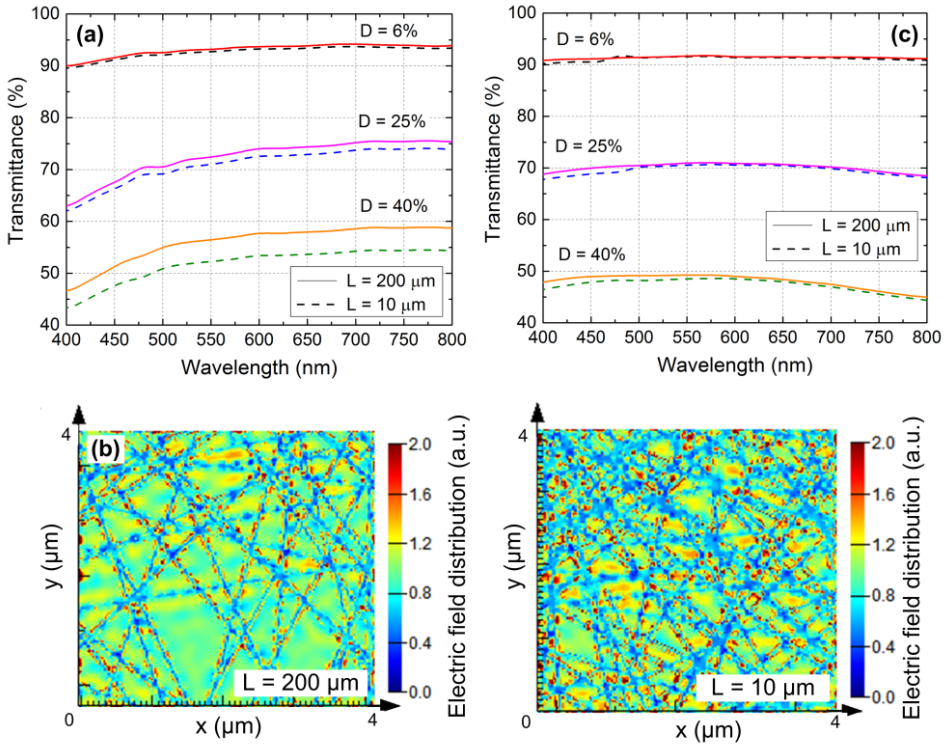

Fig. 3. (a) Transmittance spectra of AgNW films for various coverage densities *D* and lengths *L* of NWs. (b) Calculated electric field distribution for 200 μm (left) and 10 μm (right) long AgNW films at 550 nm wavelength. (c) Transmittance spectra of AlNW films for various coverage densities *D* and length *L* of NWs. The diameter *d* of NWs is 60 nm for all cases.

Figure 4(a) shows the dependence of the sheet resistance of AgNW films on the length of NWs at various coverage densities. The dependence of the sheet resistance on the growth of NWs possesses three distinctive regions: (i) a *rapid* decrease – by a factor of 5 – for short NW lengths from 10 to 20 μm; (ii) an *intermediate* decrease – by a factor of 2.25 – from 20 to 80 μm, and (iii) a *steady* decrease – by a factor of 1.2 times – for long NWs from 80 μm to 200 μm. Thus, the length of NWs influences on the sheet resistance most significantly until 80 μm; while further lengthening affects less radical. Such behavior of the sheet resistance corresponds to the nonlinear increase of the effective number of NW crossings $\langle N_i^* \rangle$ from Eq. (2) with growth of NW length as shown in the inset of Fig. 4(a). Figure 4(b) shows the dependence of the sheet resistance of AgNW films on the diameter at the coverage density *D* = 25% and the length of NWs equal to *L* = 10, 50 and 200 μm. The sheet resistance decreases 5.8 times when diameter *d* of NWs increases from 30 to 90 nm. Nonlinear behavior results from the quadratic proportionality of the NW crossings volume V_c from Eq. (2) to diameter of NWs: $V_c \square d^2$. While thickening the diameter of NWs strongly improves the conductivity of TCFs, it also leads to significantly higher haze and thus limits the applications of TCFs on their base [48, 49]. Therefore, we conclude that NWs with longer length and thicker diameters suit more for photovoltaics, while NWs with longer length and thinner diameters – for displays and touchscreens.

Optical Materials EXPRESS

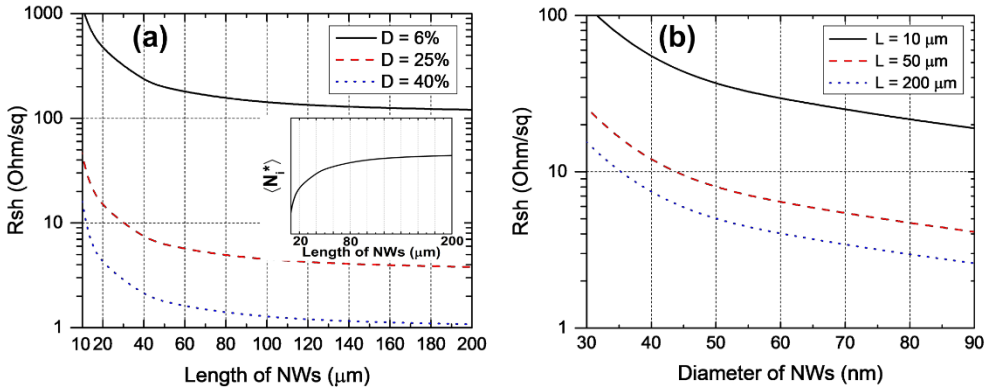

Fig. 4. (a) Sheet resistance of AgNWs films versus length of NWs for various coverage densities *D*. The diameter of NWs is 60 nm. (b) Sheet resistance of AgNWs films versus diameter of NWs for various length *L*. The coverage density *D* is 25%.

4 Conclusions

We investigated the dependence of optoelectronic properties of AgNW TCFs on the length of NWs in a broad range from 10 to 200 μm. We showed that a lengthening of NWs insignificantly influences on the transmittance at coverage densities of NWs below 25%, while the sheet resistance drops *non-linearly*. Additionally, the thickening of nanowire diameters also *non-linearly* decreases the sheet resistance. We concluded that NWs with longer length and thicker diameters suit more for photovoltaics, while NWs with longer length and thinner diameters – for displays and touchscreens. Furthermore, we believe that this study can help to estimate the impact of AgNW length on the optoelectronic performance of TCFs for variety applications.

Funding

This project is supported by National Research Foundation of Singapore (No. NRF-CRP11-2012-01), SIMTech-NTU (2016-2017), the National Key Research and Development Program of China administrated by the Ministry of Science and Technology of China (No. 2016YFB0401702), National Natural Science Foundation of China (No. 61674074, 51402148 and 61405089), Shenzhen Peacock Team Project (No. KQTD2016030111203005), Shenzhen Innovation Project (No. JCYJ20160301113356947, JCYJ20160301113537474, JCYJ20150630145302223), Foshan Innovation Project (No. 2014IT100072). XWS also thanks the start-up fund from Southern University of Science and Technology.